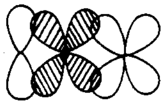

6

pair and occupied Fe(3d) orbitals for vacant phosphorus orbitals of the appropriate symmetry. Increased P–Fe π bonding should cause reduced N–P π bonding and vice versa. The fact that the average N–P bond length in $[(Me_2N)_3P]_2Fe(CO)_3$ is 0.01 Å longer than that in $(Me_2N)_3PFe(CO)_4$ is consistent with this postulate.

Acknowledgment. The authors are grateful to the National Science Foundation (Grant CHE 79-10155) and the Robert A. Welch Foundation for generous financial support. We also thank the National Science Foundation for the purchase of the Syntex P2$_1$ diffractometer (Grant GP-37028).

Registry No. 1, 40697-04-9; 2, 28382-85-6; $Fe_2(CO)_9$, 15321-51-4.

Supplementary Material Available: Listings of structure factor amplitudes and hydrogen atom parameters (45 pages). Ordering information is given on any current masthead page.

Contribution from the Department of Chemistry,
National Tsing Hua University, Hsinchu, Taiwan 300, Republic of China

Dissociation and Isomerization Kinetics of (*meso*-5,5,7,12,12,14-Hexamethyl-1,4,8,11-tetraazacyclotetradecane)copper(II) (Blue) Cation in Strongly Acidic, Aqueous Media

BIH-FONG LIANG and CHUNG-SUN CHUNG*

Received November 19, 1979

The dissociation and isomerization of the blue copper(II) complex of *meso*-5,5,7,12,12,14-hexamethyl-1,4,8,11-tetraazacyclotetradecane have been investigated spectrophotometrically in 1–5 M HNO_3. The reaction scheme

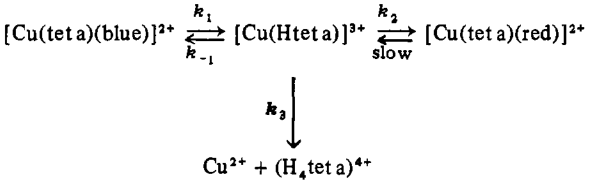

$$\begin{tikzcd}[Cu(tet\,a)(blue)]^{2+} \arrow[r, shift left, "k_1"] & {[Cu(Htet\,a)]^{3+}} \arrow[l, shift left, "k_{-1}"] \arrow[r, shift left, "k_2"] \arrow[d, "k_3"] & {[Cu(tet\,a)(red)]^{2+}} \arrow[l, shift left, "slow"] \\ & Cu^{2+} + (H_4tet\,a)^{4+} & \end{tikzcd}$$

is given, with $k_1 = (2.6\ (\pm0.3) \times 10^{-4})[H^+]\ s^{-1}\ M^{-1}$, $k_{-1} = 1.4\ (\pm0.1) \times 10^{-3}\ s^{-1}$, $k_2 = 2.5\ (\pm0.1) \times 10^{-3}\ s^{-1}$, and $k_3 = 4.6\ (\pm0.2) \times 10^{-4}\ s^{-1}$ at 25.0 °C and $\mu = 5.0$ M ($NaNO_3 + HNO_3$). The possible mechanism for the reaction and the effect of ligand cyclization are considered. The cleavage of the second copper–nitrogen bond is proposed as the rate-determining step for the dissociation reactions of $[Cu(tet\,a)(blue)]^{2+}$ and $[Cu(tet\,a)(red)]^{2+}$ in strongly acidic, aqueous media.

Introduction

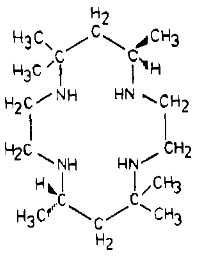

I

tet a

The macrocyclic ligand *meso*-5,5,7,12,12,14-hexamethyl-1,4,8,11-tetraazacyclotetradecane (I)[1,2] forms a blue and a red complex with copper(II).[3] The crystal structure determinations of these complexes have recently been completed.[4] The dissociation rate constants of these complexes in 6.1 M HCl reported by Cabbiness and Margerum[3] led to the discovery of the extraordinary kinetic stability of these types of complexes. In order to provide insight into the ways in which the macrocyclic ligand might impart unusual properties to the metal complexes, it was considered desirable to study the kinetics and mechanisms of the reactions of the macrocyclic complexes in strongly acidic, aqueous media. The detailed kinetic study of the dissociation and the isomerization of $[Cu(tet\,a)(blue)]^{2+}$ in 1–5 M HNO_3 (eq 1 and 2) has now been completed, and the results are reported herein.

Table I. Visible Absorption Bands at $\mu = 5.0$ M ($NaNO_3$)

complex	λ_{max}, nm	ϵ_{max}, $M^{-1}\ cm^{-1}$
$[Cu(tet\,a)(blue)]^{2+}$	615	195
$[Cu(tet\,a)(red)]^{2+}$	500	124

$$[Cu(tet\,a)(blue)]^{2+} + 4H^+ \rightarrow Cu^{2+} + (H_4tet\,a)^{4+} \quad (1)$$

$$[Cu(tet\,a)(blue)]^{2+} \rightarrow [Cu(tet\,a)(red)]^{2+} \quad (2)$$

In eq 2 structures have been determined for crystalline forms of the reactant and of the product.[4] Therefore, it is possible to be quite specific about the rearrangements that accompany the color change with $[Cu(tet\,a)]^{2+}$. The kinetics of the blue-to-red conversion of $[Cu(tet\,a)]^{2+}$ in basic solution has recently been studied in detail.[5] It is most interesting that

---

(1) Curtis, N. F. *J. Chem. Soc.* **1964**, 2644.
(2) Curtis, N. F. *Coord. Chem. Rev.* **1968**, *3*, 3.
(3) Cabbiness, D. K.; Margerum, D. W. *J. Am. Chem. Soc.* **1969**, *91*, 6540; **1970**, *92*, 2151.
(4) Clay, R. M.; Murray-Rust, P.; Murray-Rust, J. *J. Chem. Soc., Dalton Trans.* **1979**, 1135.
(5) Liang, B.-F.; Chung, C.-S. *Inorg. Chem.* **1980**, *19*, 1867.

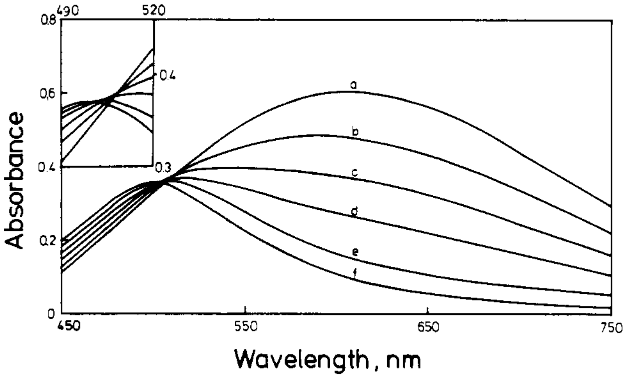

Figure 1. Change in absorption spectra during the consecutive–concurrent dissociation and isomerization of $[Cu(tet\,a)(blue)]^{2+}$ in 3.0 M HNO_3 ($\mu = 5.0$ M) at 25.0 °C. Downward from curves a to f at 615 nm, reaction times are 1.5, 7, 13, 20, 35, and 50 min. The smaller graph, in the insert, is an expansion of the part of the larger graph from 490 to 520 nm.

this reaction (eq 2) is catalyzed by acid as well as by base.

Experimental Section

Reagents. The macrocyclic ligand (tet a) was prepared by using the procedure described by Hay, Lawrance, and Curtis.[6] The complex $[Cu(tet\,a)(blue)](ClO_4)_2$ was obtained by using the method described by Hay and Clark.[7] Anal. Calcd for $CuC_{16}H_{36}N_4{\cdot}2ClO_4$: C, 35.13; H, 6.59; N, 10.25; Cl, 12.99. Found: C, 35.33; H, 6.72; N, 10.23; Cl, 12.90. $[Cu(tet\,a)(red)](ClO_4)_2$ was prepared by the procedure given by Cabbiness.[8] Anal. Calcd for $CuC_{16}H_{36}N_4{\cdot}2ClO_4$: C, 35.13; H, 6.59; N, 10.25; Cl, 12.99. Found: C, 34.98; H, 6.66; N, 10.37; Cl, 13.00. All other chemicals used in this work were Merck GR grade.

Kinetic Measurements. Kinetic runs were initiated by mixing a freshly prepared $[Cu(tet\,a)(blue)](ClO_4)_2$ solution with a solution that contained the desired quantities of HNO_3 and $NaNO_3$. All samples were then well mixed and transferred to a thermostated quartz cell. These reactions were followed spectrophotometrically by repetitive scanning through the range 450–750 nm, with particular focus on 615 nm (a maximum for $[Cu(tet\,a)(blue)]^{2+}$) and 536 nm. A Cary 17 recording spectrophotometer was used and the temperature maintained at 25.0 ± 0.1 °C for all the solutions studied. The rate constants were obtained by using the IBM 1130 computer.

Results

The visible absorption spectra were used to observe the reactions. The principal absorption bands and molar absorptivities of $[Cu(tet\,a)(blue)]^{2+}$ and $[Cu(tet\,a)(red)]^{2+}$ in 5.0 M $NaNO_3$ at 25.0 °C are given in Table I.

The dissociation process of $[Cu(tet\,a)(blue)]^{2+}$ (eq 1) was found not to occur by a single stage but to take place in consecutive steps. The isomerization of $[Cu(tet\,a)(blue)]^{2+}$ (eq 2), which occurs concurrently with its dissociation, provided additional evidence for the complexity of these reactions. These features are illustrated by a typical set of scans in 3.0 M HNO_3 shown in Figure 1 and the absorbance vs. time profiles shown in Figure 2. The simplest kinetic scheme (eq 3) that can accommodate our observations involves consecutive–concurrent first-order processes with reversible steps. A,

$$\begin{tikzcd}
A \arrow[r, shift left, "k_1"] & B \arrow[l, shift left, "k_{-1}"] \arrow[r, shift left, "k_2"] \arrow[d, "k_3"] & C \arrow[l, shift left, "k_{-2}"] \\
& D &
\end{tikzcd} \tag{3}$$

B, C, and D are respectively $[Cu(tet\,a)(blue)]^{2+}$, an intermediate, $[Cu(tet\,a)(red)]^{2+}$, and $Cu^{2+} + (H_4tet\,a)^{4+}$, and k_1, k_{-1}, k_2, k_{-2}, and k_3 are first-order or pseudo-first-order rate constants. The value of k_{-2}, obtained by measuring the dissociation rate of $[Cu(tet\,a)(red)]^{2+}$ in 1–5 M HNO_3, is much smaller than any of the other resolved rate constants. During the first 80% of the reaction, k_{-2} can be neglected. The approximate values of the rate constants were estimated from kinetic measurements. The approximate molar absorptivity of B, ϵ_B, was guessed from scanning spectra. Rodiguin and Rodiguina integration[9] would give the values of the concentrations of A, B, C, and D as a function of time. A comparison of the calculated values of absorbances with the observed values, followed by a variation of the rate constants and ϵ_B so as to obtain a minimum deviation between observed and calculated values, would lead to the correct rate constants. The value of ϵ_B at 536 nm, evaluated with the use of computer programs, is 165 ± 20 $cm^{-1}\,M^{-1}$ in the range 1.0–5.0 M HNO_3. Resulting values of these rate constants are given in Table II. One of these experimental curves and the best fit curve in 3.0 M HNO_3, calculated with the rate constants listed in Table II, are shown in Figure 2. The other curves in the range 1.0–5.0 M HNO_3 are very similar to this particular curve shown in Figure 2.

The results given in Table II indicate that k_1 is the only $[H^+]$-dependent rate constant. A plot of k_1 against $[H^+]$ gives

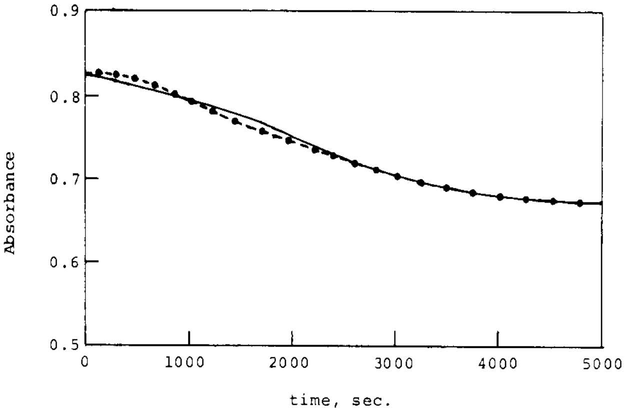

Figure 2. Absorbance vs. time for the reaction of $[Cu(tet\,a)(blue)]^{2+}$ in 3 M HNO_3 ($\mu = 5.0$ M) at 536 nm and 25.0 °C. The solid line is the experimental curve, and the dashed line is the best fit curve calculated with the constants listed in Table II.

Table II. Consecutive–Concurrent First-Order Rate Constants for the Dissociation and Isomerization of $[Cu(tet\,a)(blue)]^{2+}$ Cation at 25.0 °C and $\mu = 5.0$ M (HNO_3 + $NaNO_3$)

$[HNO_3]$, M	10^4k_1, s^{-1}	10^3k_{-1}, s^{-1}	10^3k_2, s^{-1}	10^4k_3, s^{-1}
1.0	2.6	1.5	2.5	4.4
1.5	3.9	1.5	2.5	4.4
2.0	5.6	1.4	2.4	4.4
2.5	6.3	1.4	2.4	4.5
3.0	7.6	1.4	2.5	4.5
3.5	9.0	1.4	2.4	4.6
4.0	10.8	1.3	2.5	4.7
4.5	11.8	1.3	2.4	4.7
5.0	13.4	1.3	2.5	4.8

Table III. Pseudo-First-Order Rate Constants as a Function of Acid Concentration at 25 °C and $\mu = 5.0$ M (HNO_3 + $NaNO_3$)

$k_1 = 2.6\ (\pm 0.3) \times 10^{-4}[H^+]\ s^{-1}\,M^{-1}$ $k_2 = 2.5\ (\pm 0.1) \times 10^{-3}\ s^{-1}$
$k_{-1} = 1.4\ (\pm 0.1) \times 10^{-3}\ s^{-1}$ $k_3 = 4.6\ (\pm 0.2) \times 10^{-4}\ s^{-1}$

---

(6) Hay, R. W.; Lawrance, A. G.; Curtis, N. F. *J. Chem. Soc., Perkin Trans. 1* **1975**, 591.

(7) Hay, R. W.; Clark, C. R. *J. Chem. Soc., Dalton Trans.* **1977**, 1148.

(8) Cabbiness, D. K. Ph.D. Thesis, Purdue University, **1970**.

(9) Rodiguin, N. M.; Rodiguina, E. N. "Consecutive Chemical Reactions"; Van Nostrand: Princeton, N.J., 1964.

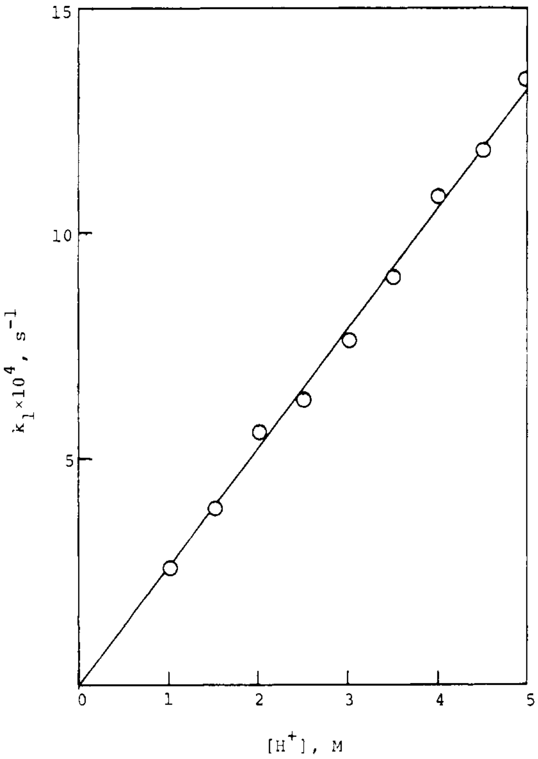

Figure 3. Plot of k_1 against [H$^+$].

a straight line with slope 2.6×10^{-4} M^{-1} s^{-1} as shown in Figure 3. The values for the pseudo-first-order rate constants as a function of acid concentration at 25.0 °C and μ = 5.0 M (HNO_3 + $NaNO_3$) are listed in Table III.

Discussion

The crystal structure determinations of [Cu(tet a)(blue)]$^{2+}$ and [Cu(tet a)(red)]$^{2+}$ have recently been completed.[4] The blue species differs from the red species only in the configuration of a single chiral nitrogen center.[4] This difference and the isomerization of [Cu(tet a)(blue)]$^{2+}$, which occurs concurrently with its dissociation, suggest that B is an intermediate where one metal–amine bond is broken.

The rate constant for the dissociation of [Cu(tet a)(blue)]$^{2+}$ is much faster than that for the dissociation of [Cu(tet a)(red)]$^{2+}$. This difference is mainly due to the fact that [Cu(tet a)(blue)]$^{2+}$ contains unstable chelate rings. In the case of the red tet a complex, the ligand is in its most stable configuration, with both six-membered chelate rings in a chair form and both five-membered chelate rings in a gauche form.[10]

A general accepted mechanism for the dissociation of metal–polyamine chelates proposed by Margerum[11] will readily explain the observed rate equations for these dissociations. For the purposes of visualization, therefore, we have represented in Figure 4 the stepwise mechanism, where species 1, 3, and 5 are [Cu(tet a)(blue)]$^{2+}$, intermediate B, and [Cu(tet a)(red)]$^{2+}$, respectively. In strongly acidic media, $k_{23}[H^+] \gg k_{21}$ and $k_{43}[H^+] \gg k_{45}$, so that $k_1 = k_{13}[H^+] + k_{12}$, $k_{-1} = k_{21}k_{32}/k_{23}[H^+] + k_{31}$, $k_2 = k_{45}k_{34}/k_{43}[H^+] + k_{35}$, and $k_3 = k_{37}[H^+] + k_{36}$. In 1–5 M HNO_3, the experimental results indicate that k_1 is the only [H$^+$]-dependent rate constant, so that $k_{12} \ll k_{13}[H^+]$, $k_{21}k_{32}/k_{23}[H^+] \ll k_{31}$, $k_{45}k_{34}/k_{43}[H^+] \ll k_{35}$, and $k_{37}[H^+] \ll k_{36}$. The values for the resolved rate constants are listed in Table IV.

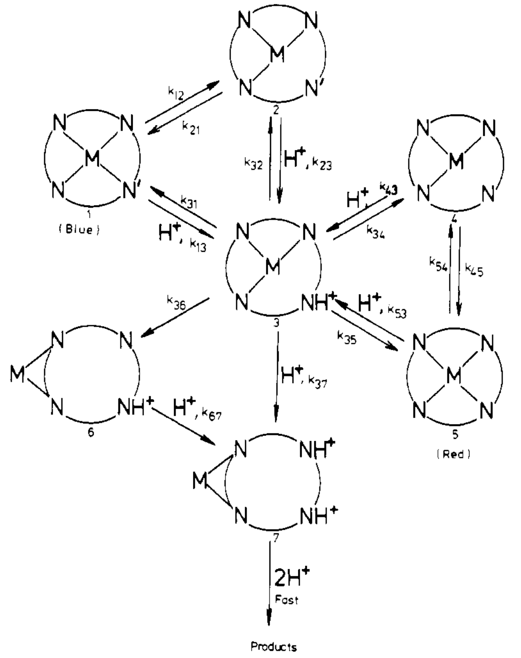

Figure 4. Proposed stepwise mechanism for the dissociation and isomerization of [Cu(tet a)(blue)]$^{2+}$ in strongly acidic media.

Table IV. Resolved Rate Constants for the Dissociation and Isomerization of [Cu(tet a)(blue)]$^{2+}$ at 25.0 °C and μ = 5.0 M (HNO_3 + $NaNO_3$)

$k_{13} = 2.6\ (\pm 0.3) \times 10^{-4}\ s^{-1}\ M^{-1}$ $k_{35} = 2.5\ (\pm 0.1) \times 10^{-3}\ s^{-1}$
$k_{31} = 1.4\ (\pm 0.1) \times 10^{-3}\ s^{-1}$ $k_{36} = 4.6\ (\pm 0.2) \times 10^{-4}\ s^{-1}$

The proposed mechanism can be modified and used in the case of the dissociation reactions of complexes of open-chain polyamines.[11] A comparison between the dissociation kinetics of the complexes of cyclic and open-chain polyamines can provide an insight into the effect of ligand cyclization. The breaking of the first copper–nitrogen bond, step 1 to 2 or step 1 to 3, involves some angular expansion of the bond angles in the chelate rings, resulting in much larger activation energies for macrocyclic complexes than for the complexes of the linear polyamines. In the case of the complexes of open-chain polyamines, the breaking of the first copper–nitrogen bond involves the formation of an intermediate state with the donor group displaced from the normal chelation position. The metal ion becomes solvated, and there is rotation and protonation of the leaving donor group. The solvation of the metal ion and the protonation of the leaving amine group stabilize species 3, and so k_{-1} is smaller than k_3 in strongly acidic, aqueous media. Therefore, the rate-determining step in strong acid is the breakage of the first copper–nitrogen bond for the complexes of open-chain polyamines.[12] In the case of a macrocyclic complex, after the breaking of the first copper–nitrogen bond, step 1 to 2 or step 1 to 3, the macrocyclic ligand twists or folds instead of internally rotating the leaving group. The uncoordinated amine group and the metal ion are very close, and the solvation of the metal ion is sterically hindered to a large extent, with the result that k_{-1} is larger than k_3. Therefore, the breakage of the second copper–nitrogen bond is proposed as the rate-determining step for the dissociation reactions of the macrocyclic complexes in strongly acidic, aqueous media. This is in marked contrast to the kinetics of the complexes of the open-chain polyamines. From the above

---

(10) Whimp, P. O.; Bailey, M. F.; Curtis, N. F. *J. Chem. Soc. A* **1970**, 1956.

(11) Margerum, D. W.; Rorabacher, D. B.; Clarke, J. F. G., Jr. *Inorg. Chem.* **1963**, *2*, 667.

(12) Margerum, D. W.; Cayley, G. R.; Weatherburn, D. C.; Pagenkopf, G. K. *ACS Monogr.* **1978**, *No. 174*.

discussion, we may conclude that ligand cyclization makes impossible the rotation of the uncoordinated amine group of the reaction intermediates from the vicinity of the metal ion, resulting in the retardation of the protonation of the uncoordinated amine group, the retardation of the breakage of the copper–nitrogen bond, the acceleration of the deprotonation of the uncoordinated amine group, and the acceleration of the formation of the copper–nitrogen bond. These effects can throw light on the kinetic and thermodynamic properties of macrocyclic compounds.

In the isomerization reaction (eq 2), crystal structure determinations of the reactant and the product indicate that one of the four nitrogens must be inverted during this reaction. In strongly acidic media, this reaction is acid catalyzed due to the required cleavage of one copper–nitrogen bond as shown in Figure 4. It is most interesting that this blue-to-red interconversion in basic solution is base catalyzed.[5] In contrast to the isomerization in acidic media, the base-catalyzed configurational conversion occurs while the ligand is coordinated, and a concerted mechanism is proposed for the reaction of coordinated hydroxide ion with amine hydrogens.[5,13]

Acknowledgment. This work was supported by a grant from the Chemistry Research Center, National Science Council of the Republic of China, to which the authors wish to express their thanks.

Registry No. $[Cu(tet\,a)(blue)]^{2+}$, 73464-68-3; $[Cu(tet\,a)(red)]^{2+}$, 73464-69-4.

---

(13) Liang, B.-F.; Margerum, D. W.; Chung, C.-S. *Inorg. Chem.* **1979**, *18*, 2001.

Contribution from the School of Chemistry,
The University of New South Wales, Kensington, New South Wales 2033, Australia

The Zinc–Benzenethiolate–Halide System. Synthesis and Structure of the Hexakis(μ-(benzenethiolato))-bis(benzenethiolato)dichlorotetrazincate(II) Dianion

IAN G. DANCE

Received July 1, 1980

The crystallization of complexes $(Me_4N)_2[Zn_4(SPh)_8X_2]$ (X = Cl, Br), $(Me_4N)_2[Zn_4(SPh)_9Cl]$, and $(Me_4N)_2[Zn_4(SPh)_{10}]$ from alcohol–acetone solutions containing solvated zinc(II), benzenethiolate, and halide ions is described and interpreted in terms of equilibria involving these and other species. The adamantane cage structure of $[(\mu\text{-}SPh)_6(ZnSPh)_4]^{2-}$ occurs also in $[(\mu\text{-}SPh)_6(ZnSPh)_2(ZnX)_2]^{2-}$ (X = Cl, Br (isostructural)) with two terminal halide ligands. No evidence for halide substitution of more than two terminal positions has been obtained. Slight distortions of the adamantane cage, principally in the positions of the bridging sulfur atoms, are associated with differentiated phenyl ring orientations, not the chloride substitution which has no detectable influence on the geometry of the cage. Mean distances are $Zn\text{–}S(Cl)_{terminal} = 2.257 \pm 0.007$ and $Zn\text{–}S_{bridging} = 2.358 \pm 0.005$ Å. Crystal data: $a = 12.377$ (2) Å, $b = 16.592$ (3) Å, $c = 16.967$ (3) Å, $\alpha = 76.68$ (1)°, $\beta = 69.92$ (1)°, $\gamma = 72.57$ (1)°, $P\bar{1}$, $Z = 2$, 4138 observed reflections, $R = 0.052$.

Introduction

Exploratory research on the coordination chemistry intrinsic to the fundamental thiolate donor function RS^-, as manifest in homoleptic metal thiolate complexes $[M_x(SR)_y]$ and complexes in which thiolate ligands predominate, has revealed new patterns of complex formation and structure. General results relevant to the observations described in this paper include the following: (i) monometallic complexes $[M(SR)_4]^{2-}$ and tetrametallic complexes $[M_4(SR)_{10}]^{2-}$, both with tetrahedral metal coordination, exist in solution equilibria and can be isolated;[1-5] (ii) the adamantane cage structure $[(\mu\text{-}SR)_6(MSR)_4]$ is ubiquitous;[1-5] (iii) solvent coordination is significant only in systems with $Zn(SPh)_2$ stoichiometry, and there exist solvent dependent reactions interconverting structurally molecular and structurally nonmolecular compounds;[2] (iv) halide coordination appears not to be competitive with benzenethiolate coordination in complexes of Cu(I), Ag(I), Sn(IV), or Pb(II),[6-9] but mixed pentafluorobenzenethiolate–chloride complexes are known;[10] (v) an internal spherical halide ligand can provide structural stability for a large cage;[11] (vi) despite the pseudohalide characteristics of the thiolate function, the formulations and structures of homoleptic metal thiolate cage complexes have no precedent in metal halide complexes.

A question that arises from these generalizations is whether terminal ligand positions on the adamantane cage structure can be substituted by halide (X), or by solvent or other uncharged ligands (L), in complexes $[(\mu\text{-}SR)_6(MSR)_{4-n}(MX)_n]^{2-}$ or $[(\mu\text{-}SR)_6(MSR)_{4-n}(ML)_n]^{n-2}$ (n = 1–4). This paper describes the crystallization of adamantane cage complexes from solutions containing Zn^{2+}, PhS^-, and Cl^- or Br^-. Conditions for crystallization of the disubstituted cage $[(\mu\text{-}SPh)_6(ZnSPh)_2(ZnX)_2]^{2-}$ (X = Cl, Br) with Me_4N^+ have been defined, and the structure of this cage has been determined by diffraction analysis. Solutions of this type crystallize also the unsubstituted cage, in $(Me_4N)_2[(\mu\text{-}SPh)_6(ZnSPh)_4]$, and a compound which probably contains the monosubstituted

---

(1) Dance, I. G. *J. Am. Chem. Soc.* **1979**, *101*, 6264.
(2) Dance, I. G. *J. Am. Chem. Soc.* **1980**, *102*, 3445.
(3) Swenson, D; Baenziger, N. C; Coucouvanis, D. *J. Am. Chem. Soc.* **1978**, *100*, 1932. Coucouvanis, D., private communication, 1980.
(4) Dance, I. G.; Guerney, P. J.; Zimmermann, W., unpublished work on $[Cd(SPh)_4]^{2-}$ and $[Cd_4(SPh)_{10}]^{2-}$.
(5) Hagen, K. S.; Berg, J. M.; Holm, R. H. *Inorg. Chim. Acta* **1980**, *45*, L17.
(6) Halide ligands are not present in complexes crystallized from a variety of solutions containing both halide and benzenethiolate.[7-9]
(7) Dance, I. G.; Calabrese, J. C. *Inorg. Chim. Acta* **1976**, *19*, L41.
(8) Dance, I. G. *Aust. J. Chem.* **1978**, *31*, 2195.
(9) Dance, I. G.; Katende, S.; Calabrese, J. C., to be published.
(10) Muller, M.; Clark, R. J. H.; Nyholm, R. S. *Transition Met. Chem.* **1978**, *3*, 369.
(11) Dance, I. G. *J. Chem. Soc., Chem. Commun.* **1980**, 818.

0020-1669/81/1320-2155$01.25/0